ISSN 0915-633X

NATIONAL INSTITUTE FOR FUSION SCIENCE

Magnetic Surface Breaking in 3D MHD Equilibria of $\ell=2$ Heliotron

T. Hayashi, A. Takei and T. Sato

(Received – Dec. 21, 1991)

NIFS-130 Jan. 1992

RESEARCH REPORT
NIFS Series

This report was prepared as a preprint of work performed as a collaboration research of the National Institute for Fusion Science (NIFS) of Japan. This document is intended for information only and for future publication in a journal after some rearrangements of its contents.

Inquiries about copyright and reproduction should be addressed to the Research Information Center, National Institute for Fusion Science, Nagoya 464-01, Japan.

NAGOYA, JAPAN

MAGNETIC SURFACE BREAKING IN 3D MHD EQUILIBRIA OF l=2 HELIOTRON

Takaya Hayashi, Akira Takei and Tetsuya Sato
National Institute for Fusion Science, Nagoya 464-01, Japan

ABSTRACT

Magnetic surface breaking due to the finite pressure effect is analyzed for three dimensional magnetohydrodynamic equilibria of l=2 Heliotron configuration. Characteristics of magnetic island formation are extensively surveyed. It is found that the well-hill criterion which has been predicted by the local analysis is not always applicable for all cases.

keywords; helical system, Heliotron, 3D MHD equilibrium, magnetic surface breaking, finite pressure effect, equilibrium beta limit, vertical field, quadrupole field, hexapole field, l=1 coil, magnetic island

1 Introduction

That magnetic surfaces can be deteriorated by finite pressure effects in toroidal helical systems has long been known ,[1-3] but there has been no practical quantitative method to investigate this phenomenon. Recently developed three dimensional equilibrium code, HINT ,[4] is dedicated for its analysis. As is described in the previous paper ,[5,6] an important discovery obtained by the code is that breaking of magnetic surfaces occurs in actual configurations of toroidal helical systems such as the Heliotron (or Torsatron) configuration. Namely, the outer ergodic region, which is observed even in the vacuum field due to the loss of symmetry, expands and the plasma region shrinks when the plasma beta is increased. What should be noted is that such breaking of magnetic surfaces due to finite pressure effects often imposes severer limitation on the equilibrium beta than the Shafranov shift.

The origin of the appearance of magnetic islands in a finite beta equilibrium of toroidal helical system is attributed to the plasma current which is induced to satisfy the equilibrium force balance condition $\mathbf{j} \times \mathbf{B} = \nabla \mathbf{p}$. The resonant field, which can be produced by the plasma current (dominant effects are given by its parallel component) in the nonaxisymmetric torus, causes appearance of magnetic islands inside the plasma. When an island is induced, the pressure profile is significantly modified near the island. Thus, a consistent analysis between the equilibrium ($\mathbf{j} \times \mathbf{B} = \nabla \mathbf{p}$) condition and the island formation is required.

As for the evaluation of the breaking of magnetic surfaces, there have been two approaches. One is to pay attention to the local effect of the plasma current, and discuss a very fine structure of pressure profile near a rational surface, whereby sizes of islands can be estimated as a saturation level of some resistive instability (local analysis) .[7-9] The local approach results in a simple criterion for the formation of magnetic islands; islands grow in a magnetic hill region, but not in a well region .[7] Our approach is dedicated to the evaluation of the global effect of the plasma current. The analysis is based on a consideration that the total effect of the plasma current integrated over the whole plasma region determines the amplitude of the resonant component of the produced magnetic fields on each rational surface. In this analysis, 3D effect of the total structure need to be taken into account consistently, which is not fully treated in the local analysis. As will be discussed in this paper, the well-hill criterion predicted by the local analysis is not clearly satisfied in the global analysis, and the results sometimes show opposite tendency in appearance. Therefore, it may be natural to consider that these two approaches deal with different physical aspects of the formation of islands, and they are

supplementary to each other.

At present there exist several excellent 3-D equilibrium codes ,[10–13] and they are actively utilized to analyze properties of helical equilibria. However, one drawback of these codes is that they assume a priori the existence of clearly nested magnetic surfaces, either explicitly or implicitly. In order to investigate the magnetic surface breaking, therefore, a new approach is invoked. Several works have thus far addressed numerical evaluation of the global effect on the breaking ,[14,15] but it remains unclarified. In order to analyze this problem quantitatively, we developed a 3D equilibrium code HINT.

In the following, we show the results obtained by using this code on Heliotron/Torsatron configurations, and study the general tendency of the island formation.

2 Magnetic Surface Breaking

Figure 1 shows an example of a process how the breaking of magnetic surfaces expands as β increases, when the operation to suppress the breaking is not carefully done. The figure shows magnetic surfaces for one typical poloidal cross section of a Heliotron configuration, with the pitch period number $M = 10$ and the pitch parameter $\gamma_c \equiv \frac{M}{l}\frac{a_c}{R_c} = 1.2$, for a vacuum field ((a)), and for a finite β equilibrium ($\bar{\beta} \sim 3.7\%$) ((b)). An ergodic region is observed on the boundary of the vacuum field. As β increases, as is shown in the enlarged figure of (b), the boundary surfaces are ergodized due to the finite pressure effect, and the size of the outermost magnetic surface defined by the last closed clear surface shrinks.

Since the calculation is executed on the finite size grid points, we have to be careful about whether the observed formation of islands is due to some numerical artifacts or not. In order to clarify this, we execute a convergence check where the same equilibrium calculation is made on the grid points with different sizes. The results are compared in Fig.2 (a) (the grid size is $49 \times 49 \times 21$ for half pitch period), and (b) ($97 \times 97 \times 29$). As can be seen in the pictures, the sizes as well as the phases of islands are very close to each other. An extrapolation of the island size for an infinite grid-size calculation gives the similar size of the island as is shown in Fig.2 (within several percent of error), which strongly supports that the results are physical.

When islands appear, the pressure profile is significantly modified. As a result of ergodization of magnetic surfaces in the boundary region, the pressure profile is peaked as is shown in Fig.3.

Here we note one property in the occurence of the breaking of magnetic surfaces; a differ-

ence between the effect of the vertical field on vacuum fields and the effect of finite pressure fields, both of which can shift the radial position of magnetic surfaces. Figure 4 (a)-(e) show the sizes of the outermost magnetic surfaces in vacuum for $l = 2/M = 10$ Heliotron configurations when the external vertical field B_v is changed to control the radial position of the magnetic axis. A noticeable property is that there exists a tight boundary, indicated with a label "breaking zone", beyond which magnetic surfaces are strongly ergodized .[16] The position of the "breaking zone" is not changed when B_v is changed, and it exists both on the outer side (as can be seen in Fig.4 (a)-(c)) and the inner side (in (c)-(e)) of the torus. The size of the outermost surface is practically determined by the surface which touches the "breaking zone", and this property is most clearly observed on the vertically elongated up-down symmetric poloidal cross section, as is shown in Fig.4. The position of the "breaking zone" does not change when other external axisymmetric fields, such as the quadrupole field B_q, are changed .[16] We observe the same property for a variety of $l = 2$ Heliotron vacuum fields with different pitch period numbers M and pitch parameters γ_c.

On the other hand, the occurence of the magnetic surface breaking in a finite pressure field has a property which is different from the vacuum one shown above. As is shown in Fig.5, the position of the boundary of the "breaking zone" for the finite pressure case becomes closer to the magnetic axis, compared with the one for the vacuum case. This can be explained by the fact that the "error" fields produced by the plasma current contain various nonaxisymmetric components, thus resulting in the expansion of the area of the noisy "breaking zone".

3 Control of Magnetic Surface Breaking

In order to understand the general tendency of the "fragility" of magnetic surfaces in a finite beta equilibrium, we have done a parameter survey for several different physical parameters. In the following, we show the effect of the pitch period number M, the external poloidal fields, and the $l = 1$ field on the occurence of the breaking.

3.1 Pitch period number M dependency

The M (pitch period number) dependency of the breaking of magnetic surfaces is shown in Fig.6 for the $l = 2$ Heliotron configuration. This survey is made under the condition that the pitch parameter γ_c is fixed to 1.3, the pressure profile is given as $p = p_0(1 - \psi)^2$ (till islands appear) where ψ is the normalized toroidal flux, and the position of the vacuum magnetic

axis is at the center of the helical coil, which is controlled by the external uniform field B_v. As is shown in Fig.6 (b), the shear and the rotational transform of the vacuum field at the plasma surface, along with the aspect ratio, increase as M increases. (It should also be noted that the magnetic hill region increases as M increases.) The tendency of magnetic surface breaking as a function of beta is shown in Fig.6 (a), where the broken line indicates a beta limit at which the outer region of about 30 % of the minor radius becomes ergodic. In general, the breaking has a tendency to be suppressed as M increases, or as the aspect ratio increases, which corresponds to restoration of the helical symmetry.

For low M (or low aspect ratio) configurations, we find that the breaking is improved by choosing other free parameters properly. The results are given in what follows.

3.2 Effect of external poloidal field

3.2.1 Effect of B_v

Figure 6 (c) shows the effect of the external vertical field B_v ,[5] which controls the radial position of the vacuum magnetic axis. As is shown here, the inward shift of the magnetic axis is favorable to suppress the breaking. In fact, by slightly shifting inward we can obtain a high beta equilibrium (such as $\bar{\beta} \geq 5\%$) for $M = 10$ configuration keeping clearly nested surfaces and the Shafranov shift limit.

The effect of B_v on the control of the breaking is visually shown in Fig.7, where an example of a finite beta equilibrium with boundary surfaces destroyed by the finite pressure effect (shown in (b)) is used as the reference ($\bar{\beta} = 3.7\%$). As is shown in Fig.7 (a), when the plasma is shifted outward by controlling B_v, the breaking remains deteriorated. On the other hand, as is shown in (c) and (d), clear surfaces recover when the plasma is shifted inward.

Thus, one practical way to control the breaking is to make use of the external vertical field B_v, which is rather easily realized by controlling the poloidal coil current in a real experiment even after the construction of the device. One problem for this way, however, is that the physical properties of the configuration, such as the rotational transform profile $\iota(r)$ and the magnetic well profile $U(r)$, are significantly modified as B_v is changed, as is shown in Fig. 8. The minor radius really increases owing to the recovery of the destroyed surfaces and the shear increases, but the well depth is noticeably reduced by the inward shift. Therefore, we have to be cautious about other physical effects, such as the stability. (We proposed a method to suppress the breaking by making use of a simple extra coil which is free from the problems

mentioned here .[17])

3.2.2 Effect of B_q

The effect of the external axisymmetric quadrupole field B_q on the breaking is shown in Fig.6 (d) .[5] In this picture, the abscissa represents the magnitude of the imposed B_q, measured in the unit of toroidally averaged magnitude of the quadrupole field produced by the helical coil current. Namely, the value of " -100% " corresponds to the case where the quadrupole component is just compensated by the external B_q, which results in a round shape of magnetic surfaces in an averaged sense. The result indicates that vertically elliptic shaping of the surfaces is favorable to suppress the breaking. Using a finite beta equilibrium with $\bar{\beta} = 2.8\%$ (shown in Fig.9) as a reference case, the effect of B_q is more clearly visualized in Fig.10 (a) for " -100% " case and (b) for " $+30\%$ " (vertically elongated) case. The corresponding change of physical properties is plotted in Fig.11 (a) and (b), respectively. The rotational transform profile is largely controlled by B_q and the well depth slightly decreases as the shape is vertically elongated. When the shape is too strongly vertically elongated by the control of B_q, the rotational transform at the magnetic axis decreases till it becomes below zero, and splitting of the axis occurs.

3.2.3 Effect of B_h

The effect of the external hexapole field B_h is shown in Fig.12, where the equilibrium shown in Fig.9 is used as a reference. In this case, " -200% " (the value is defined in the same manner as for B_q) of the hexapole field is added. The hexapole field controls the triangularity of surfaces, and the inside vertex is peaked when it is imposed negatively. We observe a slight improvement in the breaking. When the hexapole field is imposed positively, the breaking is deteriorated. However, as can be expected from the above sequence of the effect of B_v, B_q, and B_h, the ability in reduction of the breaking reduces as the pole number of the external fields increases. In fact, for a higher beta equilibrium which suffers from a wider area of ergodized boundary surfaces, it becomes difficult to suppress the breaking solely by B_h or by a higher pole number field.

3.3 Effect of l=1 field

The fact that the vertical field efficiently controls the breaking suggests that the $l = 1$ component of external fields could control the formation of islands.

In fact, when we add an $l = 1$ helical coil to the original $l = 2$ helical coils, the breaking can be remarkably controlled. A reference equilibrium with $\bar{\beta} = 3.3\%$ is shown in Fig.13 (a) for a $l = 2$ configuration. As is demonstrated in Fig.13 (b), the additional field of $l = 1$ coil (see the right panel of (b)) significantly improves the breaking, where the ratio of the $l = 1$ coil current over the $l = 2$ coil current is 0.3. The position of the $l = 1$ coil can have two kinds of phase relative to the position of the $l = 2$ coils, as is shown in the right panels of (b) and (c). It is quite interesting to note that, as is shown in Fig.13 (b) and (c), regular magnetic surfaces are remarkably recovered for both cases of the phase.

The corresponding change of the physical properties is shown in Fig.14 (a), (b), and (c), respectively. Especially, for the $l = 1$ coil field of the case of (c), the well depth increases on top of the recovery of regular magnetic surfaces, which is very favorable to the stability. (We may need to mention, however, that the particle orbit loss increases when superposing $l = 1$ coil field, case (c).)

When the direction of the $l = 1$ coil current is reversed, as is shown in Fig.15 (a), the breaking is significantly deteriorated (here, the $l = 1$ coil is the same as the case (b) in Fig.13). Furthermore, when the $l = 1$ coil current is excessively given, even if it has the proper direction, we observe deterioration in the breaking as is shown in Fig.15 (c). Thus, there exists some optimum amplitude of the $l = 1$ coil current.

4 Discussion

In this paper, we have studied the tendency of the occurence of the breaking of magnetic surfaces observed in finite beta equilibria for a variety of configurations of $l = 2$ Heliotron. These analyses are made numerically by using a 3D equilibrium code which is mainly dedicated to investigate the global effect of the plasma current. It may be interesting to summarize the results from the view point of the well-hill criterion, which was proposed in the analysis of the local-effect of the plasma current on the island formation[7] ; we observe improvement of the breaking when the configuration becomes more hill-like for the cases of M, B_v, B_q controls, and the (b)-case of $l = 1$, and when the configuration becomes more well-like for the case on the control of the (c)-case of $l = 1$. The former cases show the opposite tendency

from the well-hill criteria given by the local-effect analysis. The fact that the breaking is improved sometimes in a hill-like and sometimes in a well-like configuration suggests that the well-hill condition is not directly related to the formation of islands as for the global effect. Therefore, as we have described in the introduction, it may be natural to consider that these two approaches, namely the global and the local analyses, deal with different physical aspects of the formation of islands.

A question may arise as to why the local-effect does not apparently appear in the present calculations obtained by 3D equilibrium code. One possible answer is that a much larger grid size is required to analyze fully the local-effect up to the nonlinear stage of the relevant instability, which becomes too much expensive computations. Another possibility is that the local-effect is smaller than the global-effect in the present parameter range. (Note that the equilibrium calculation is made for a half-pitch of the torus, in which "natural islands" are analyzed, whereas the local analysis sometimes discusses about a "full-torus low-n" global mode.) A full comparison between the local and the global effect will be made in the future.

REFERENCES

[1] S.Hamada, Nucl. Fusion **2**, 23 (1962).

[2] H.Grad, Phys. Fluids **10**, 137 (1967).

[3] A.H.Reiman and A.H.Boozer, Phys. Fluids **27**, 2446 (1984).

[4] K.Harafuji, T.Hayashi, and T.Sato, J. Comput. Phys. **81**, 169 (1989).

[5] T.Hayashi, T.Sato, and A.Takei, Phys. Fluids B **2**, 329 (1990).

[6] T.Hayashi, A.Takei, N.Ohyabu, and T.Sato, in *Plasma Physics and Controlled Fusion Research* (International Atomic Energy Agency, Vienna, 1991), Vol.2, p.143.

[7] J.R.Cary and M.Kotschenreuther, Phys. Fluids **28**, 1392 (1985).

[8] C.C.Hegna and A.Bhattacharjee, Phys. Fluids B **1**, 392 (1989).

[9] C.C.Hegna, A.Bhattacharjee, Y.Nakamura, and M.Wakatani, Phys. Fluids B **3**, 2285 (1991)

[10] S.P.Hirshman and D.K.Lee, Comput. Phys. Commun. **39**, 161 (1986).

[11] F.Bauer, O.Betancourt, and P.Garabedian, *Magnetohydrodynamic Equilibrium and Stability of Stellarators* (Springer-Verlag, New York, 1984).

[12] R.Chodura and A.Schlüter, J. Comput. Phys. bf 41, 68 (1981).

[13] T.C.Hender, B.A.Carreras, L.Garcia, and J.A.Rome, J. Comput. Phys. **60**, 76 (1985).

[14] A.H.Reiman, H.S.Greenside, J. Comput. Phys. **87**, 349 (1990).

[15] W.Park, D.A.Monticello, H.Strauss, and J.Manickam, Phys. Fluids **29**, 1171 (1986).

[16] J.Todoroki, private communication (1990).

[17] T.Hayashi, A.Takei, N.Ohyabu, and T.Sato, Nucl. Fusion, **31**, 1767 (1991).

FIGURE CAPTIONS

Fig.1 Poincare plots of magnetic field lines for a $l = 2/M = 10$ Heliotron configuration, a) for a vacuum field, and b) for a finite beta equilibrium. Note that islands appear in b), as is shown in the enlarged picture, due to the finite pressure effect, and the boundary ergodic region expands.

Fig.2 Magnetic surfaces of a finite beta $l = 2/M = 10$ Heliotron equilibrium calculated on different grid sizes, (a) with $49 \times 49 \times 21$ and (b) with $97 \times 97 \times 29$ for half pitch period.

Fig.3 Pressure profile of a finite beta equilibrium of $l = 2/M = 10$ Heliotron, (a) for $\bar{\beta} = 0.7\%$, and (b) for $\bar{\beta} = 3.7\%$, at the cross section of $\phi = 18°$.

Fig.4 Vacuum magnetic surfaces of $l = 2/M = 10$ Heliotron configuration, where the position of the magnetic axis is controlled by B_v for cases (a)-(e). Note that the position of the outermost surface is practically determined by a surface just touching a boundary of an area indicated by "breaking zone", which exists on both the outer and inner side of the torus of the $\phi = 0$ cross section.

Fig.5 Position of the boundary of "breaking zone" moves into the plasma region as beta is increased. (Compare with Fig.4 for vacuum cases.)

Fig.6 General tendency of the occurence of magnetic surface breaking due to finite beta effects for $l = 2$ Heliotron configuration. (a) represents the pitch period number M dependency, and (b) is for the corresponding plasma minor radius and the rotational transform at the axis and the surface in vacuum fields when M is changed. (c) and (d) show effects of the external fields B_v and B_q, respectively.

Fig.7 Effects of B_v on the control of magnetic surface breaking.

Fig.8 The rotational transform profile and the magnetic well profile (a) before and (b) after imposing B_v (inward axis shift) to suppress magnetic islands. The plasma minor radius increases in (b) because of the recovery of outer magnetic surfaces.

Fig.9 (a) Magnetic surfaces of a $l = 2/M = 10$ Heliotron equilibria with $\bar{\beta} = 2.8\%$, where $B_q = 0$. (b) Corresponding profile of the rotational transform and the magnetic well.

Fig.10 Effects of B_q on the control of magnetic surface breaking, where (a) is with $B_q = -100\%$ and (b) with $B_q = 30\%$.

Fig.11 Corresponding profile of the rotational transform and the magnetic well for (a) and (b) of Fig.10, respectively.

Fig.12 (a) Effects of B_h on the control of magnetic surface breaking. (b) Corresponding profile of the rotational transform and the magnetic well.

Fig.13 Effects of additional $l = 1$ field on the control of magnetic surface breaking. (a) A reference equilibrium of $l = 2/M = 10$ Heliotron with $\tilde{\beta} = 3.3\%$. (b) Clear magnetic surfaces are remarkably restored when $l = 1$ field is added, where the $l = 1$ coil current is 0.3 of the $l = 2$ coil current. (c) Remarkable restoration of surfaces is also observed for the opposite phase of the $l = 1$ coil relative to the $l = 2$ coil position, as is indicated by the right panels.

Fig.14 Profiles of the rotational transform and the magnetic well, corresponding to (a),(b) and (c) of Fig.13, respectively.

Fig.15 Effects of additional $l = 1$ field on the control of magnetic surface breaking for three cases of the amplitude of the $l = 1$ coil current $I_{l=1}$, where $I_{l=1}/I_{l=2}$ is (a) -0.3 (opposite direction), (b) 0.3, and (c) 0.5.

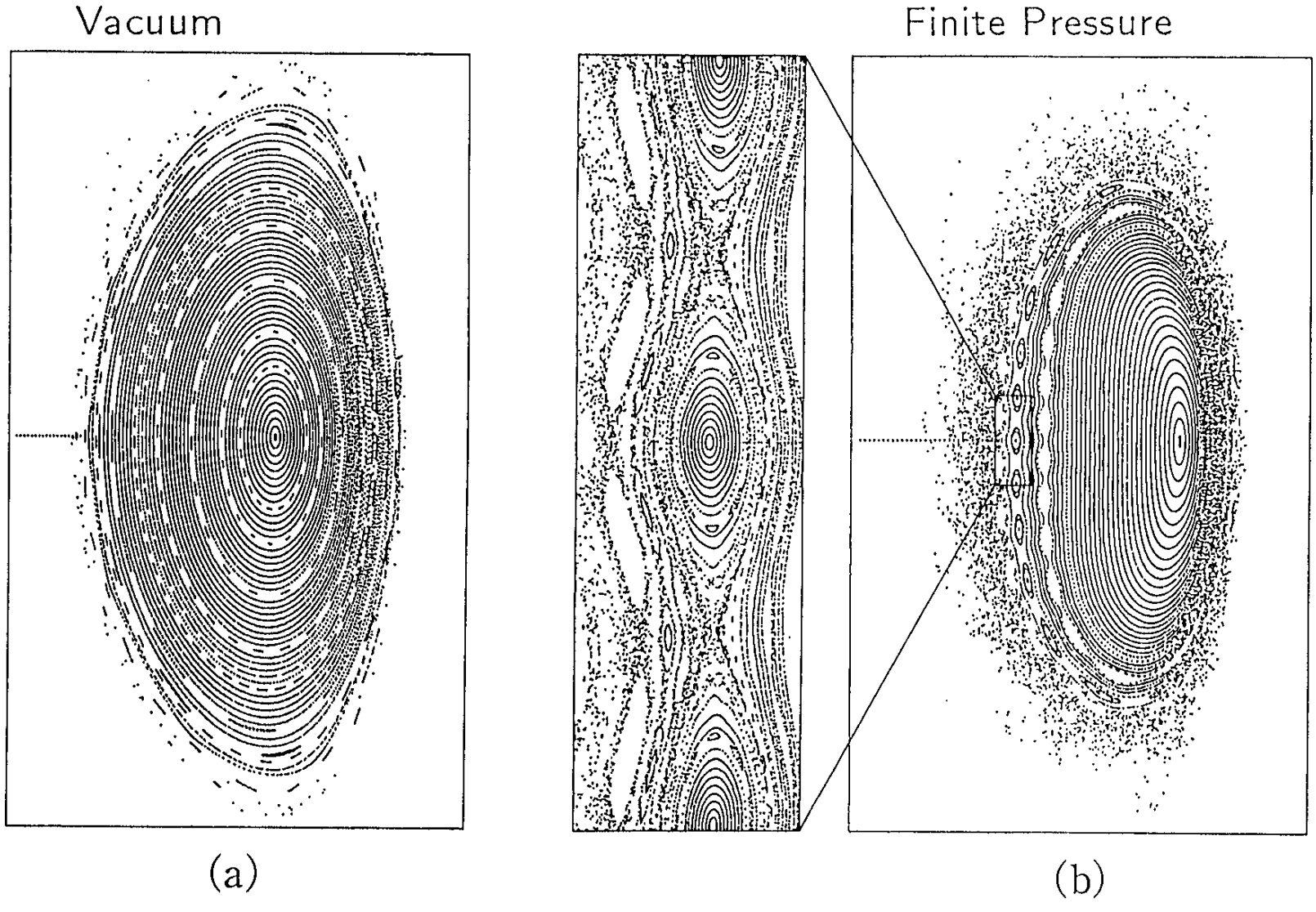

Fig.1

Mesh Convergence Check

(a) $49 \times 49 \times 21$

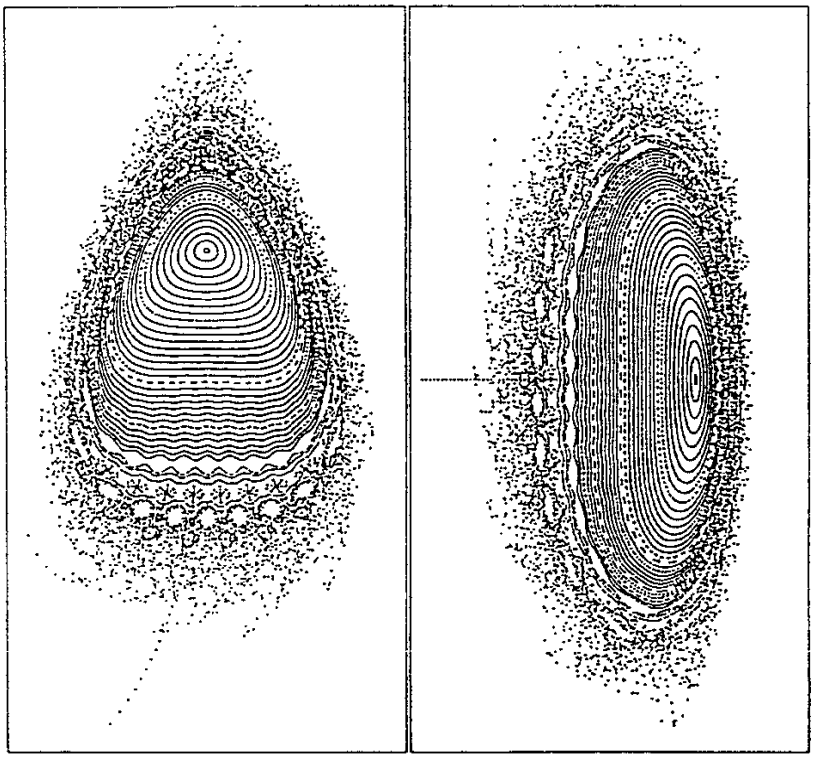

(b) $97 \times 97 \times 29$

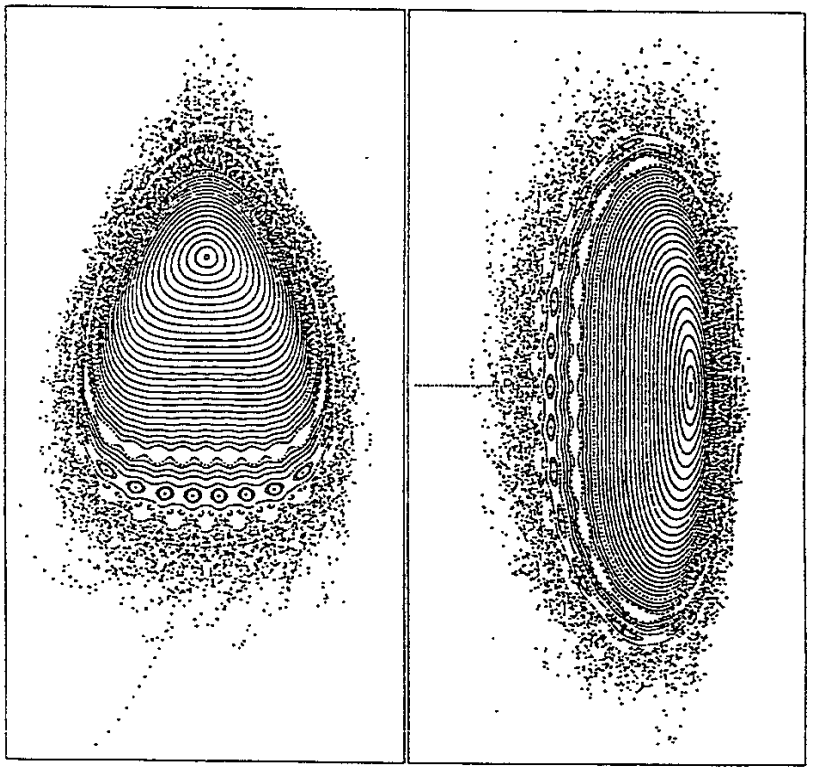

Fig.2

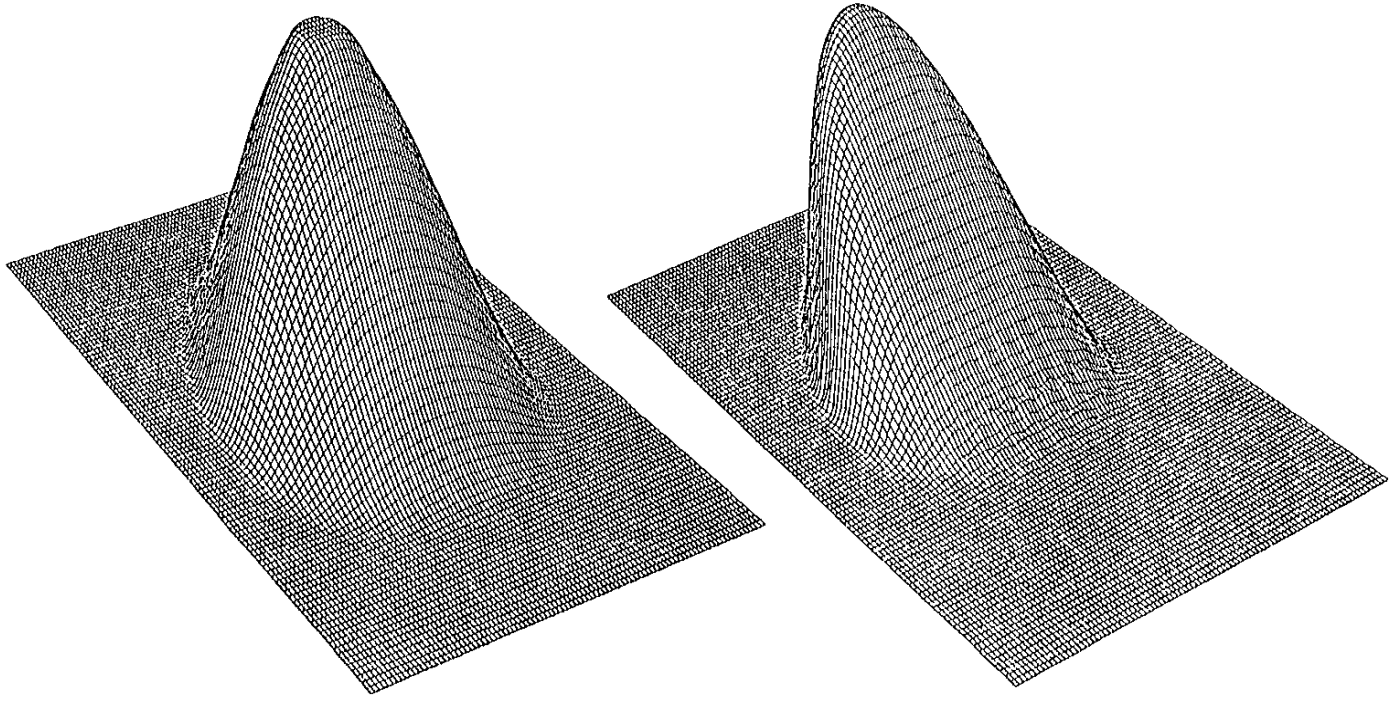

(a) (b)

Fig.3

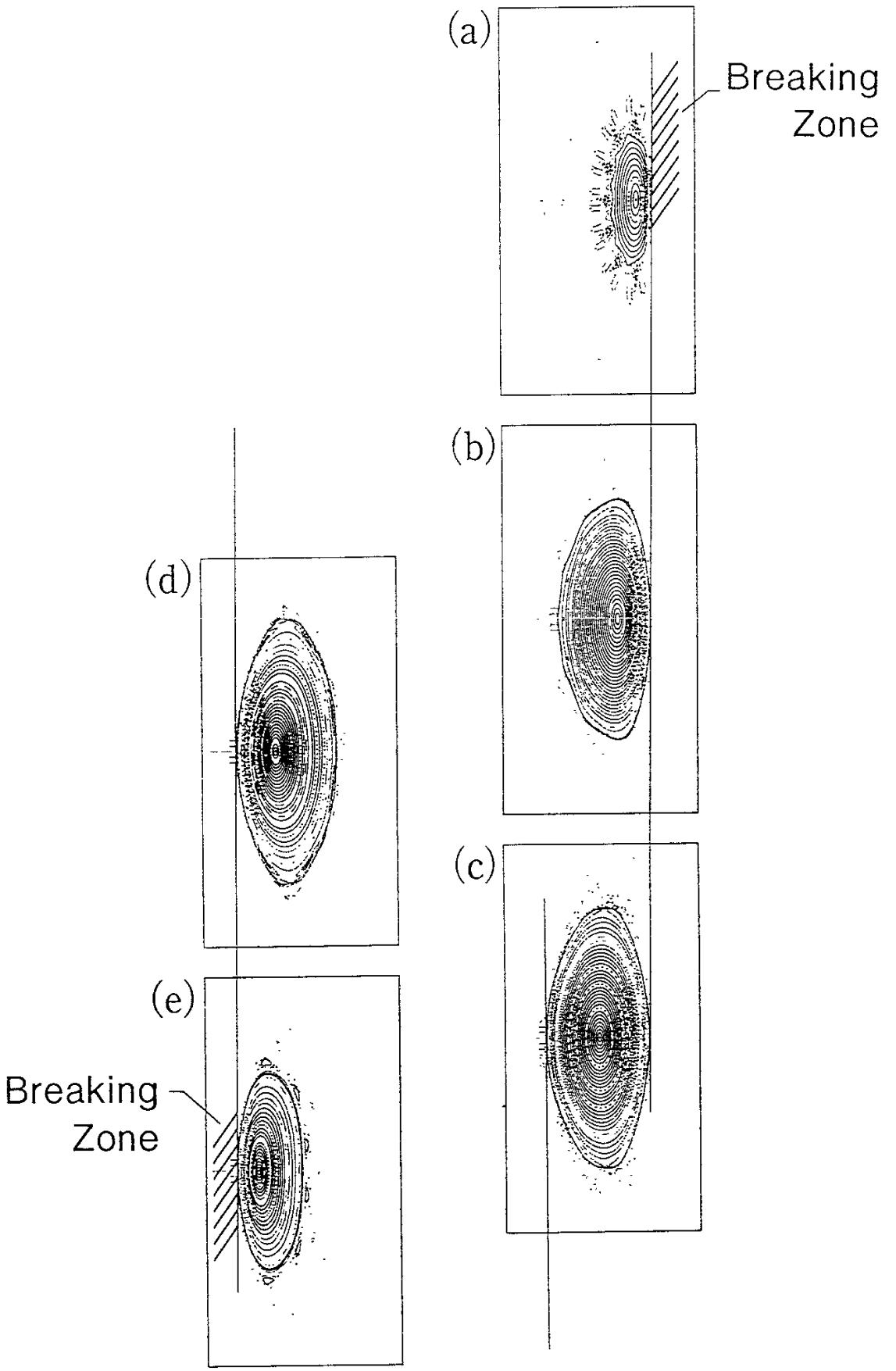

Fig.4

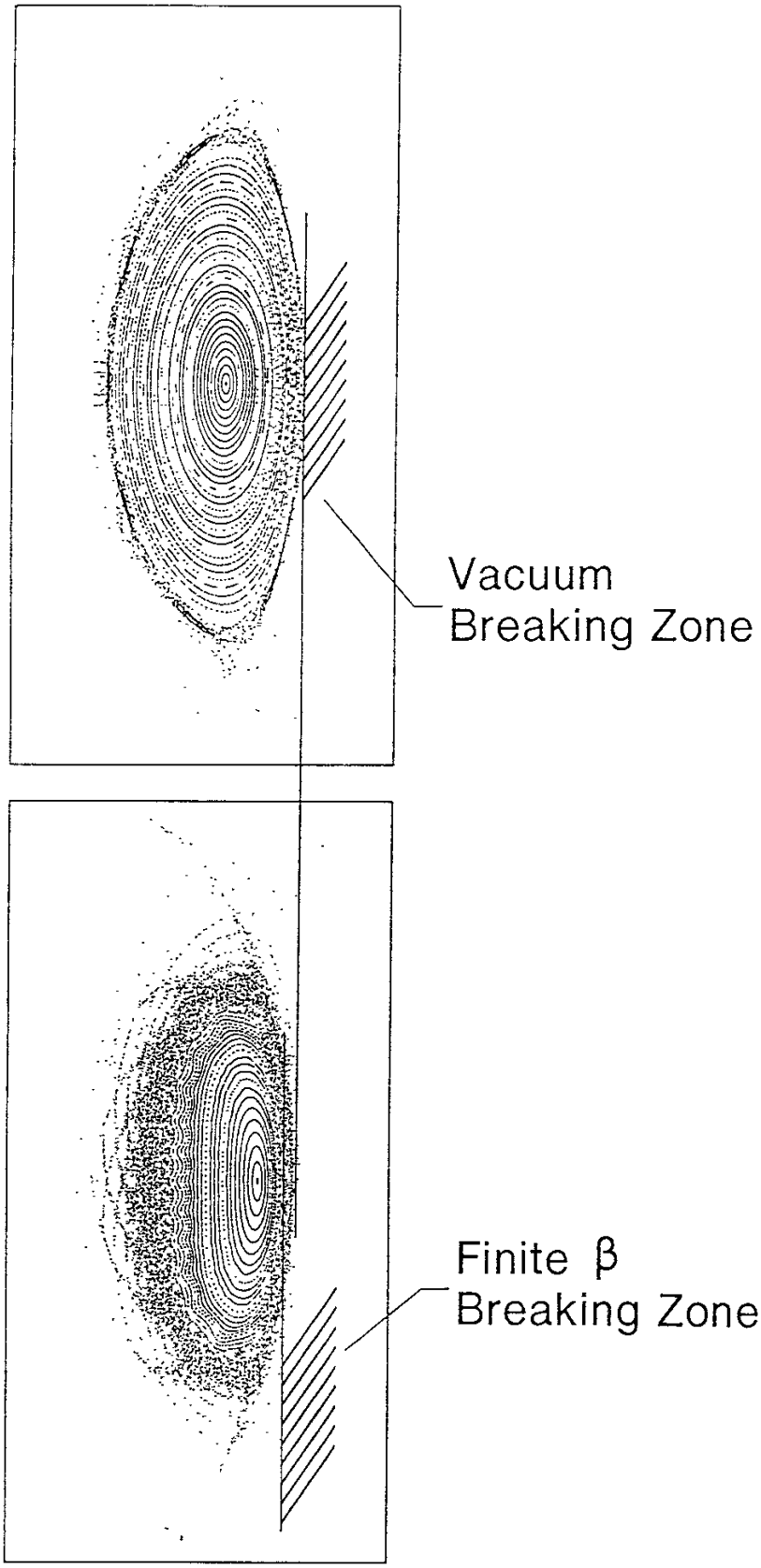

Fig.5

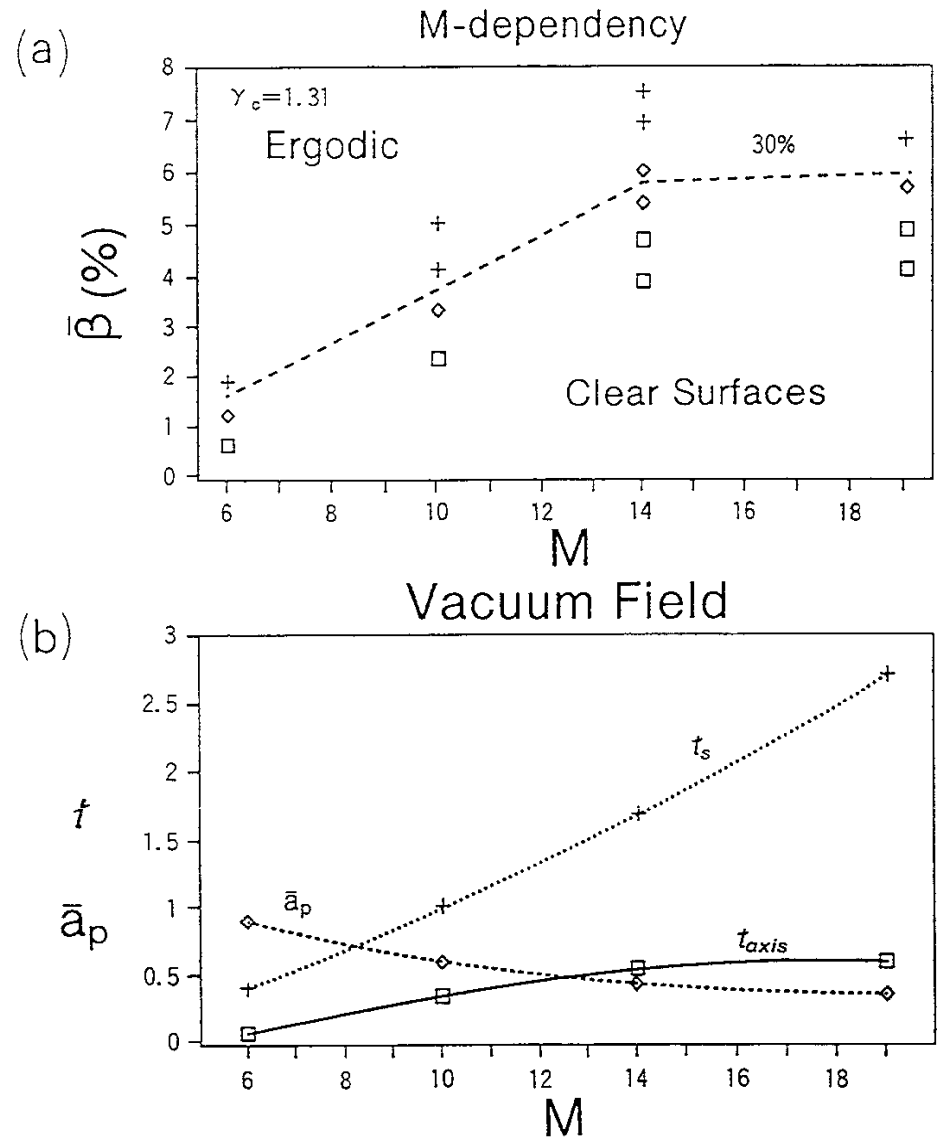
(a)
M-dependency
γ_c=1.31
Ergodic
30%
Clear Surfaces
$\bar{\beta}$ (%)
M
(b)
Vacuum Field
t_s
t_{axis}
$\bar{a}_p$
t
M

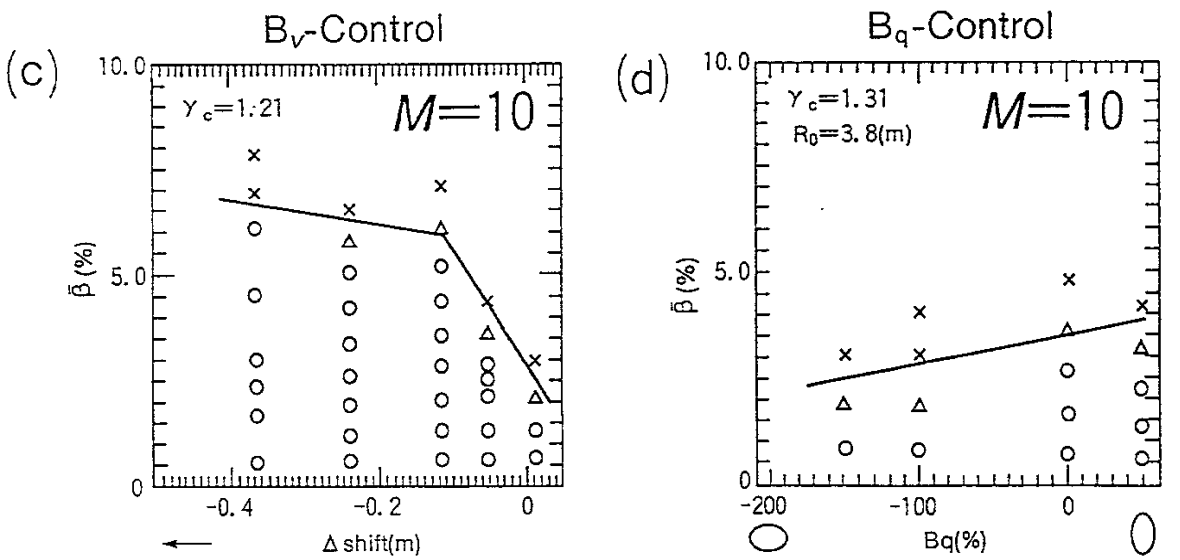
(c)
B_V-Control
γ_c=1.21
M=10
$\bar{\beta}$ (%)
Δ shift(m)
(d)
B_q-Control
γ_c=1.31
R_0=3.8(m)
M=10
$\bar{\beta}$ (%)
Bq(%)

Fig.6

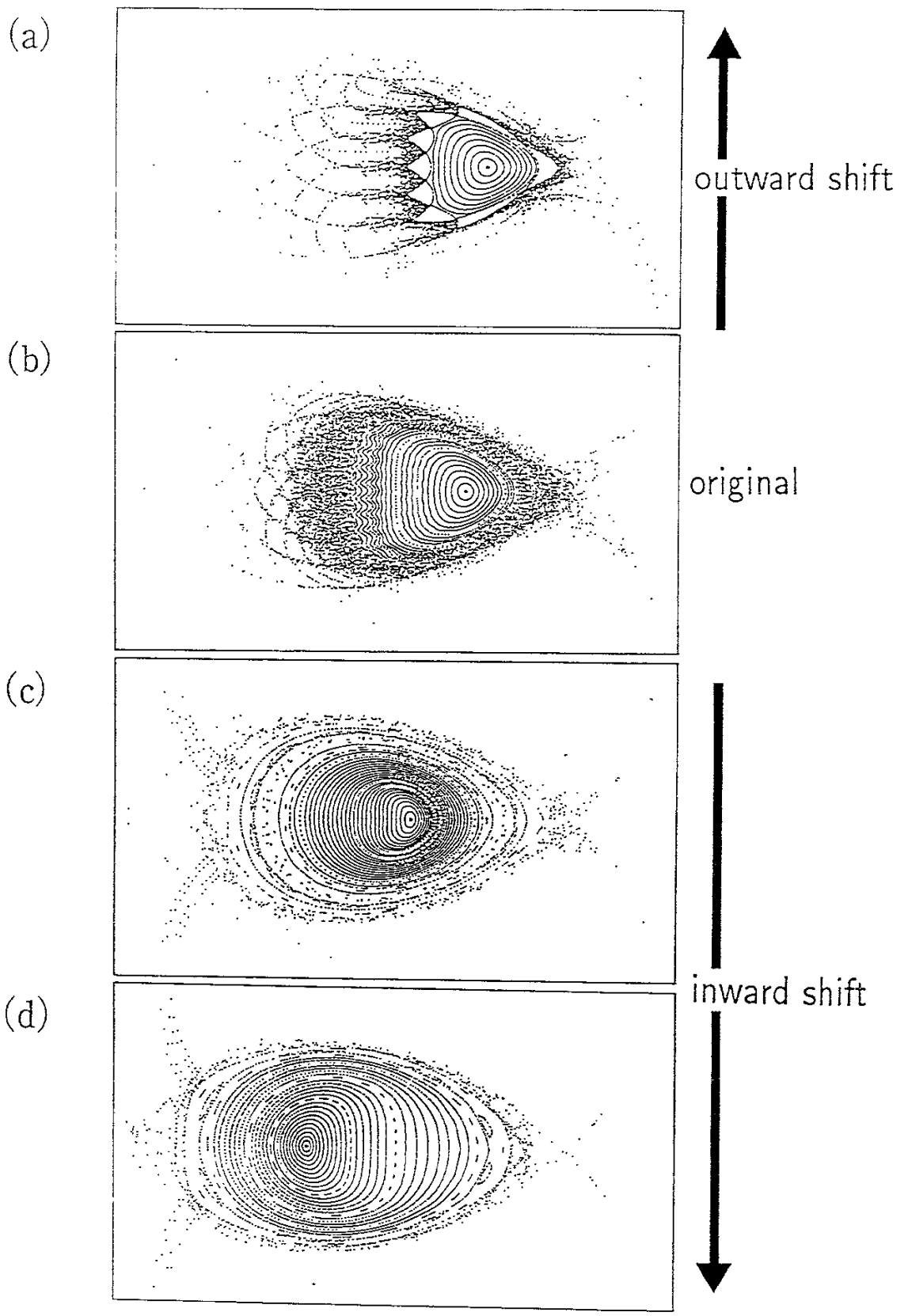

Fig.7

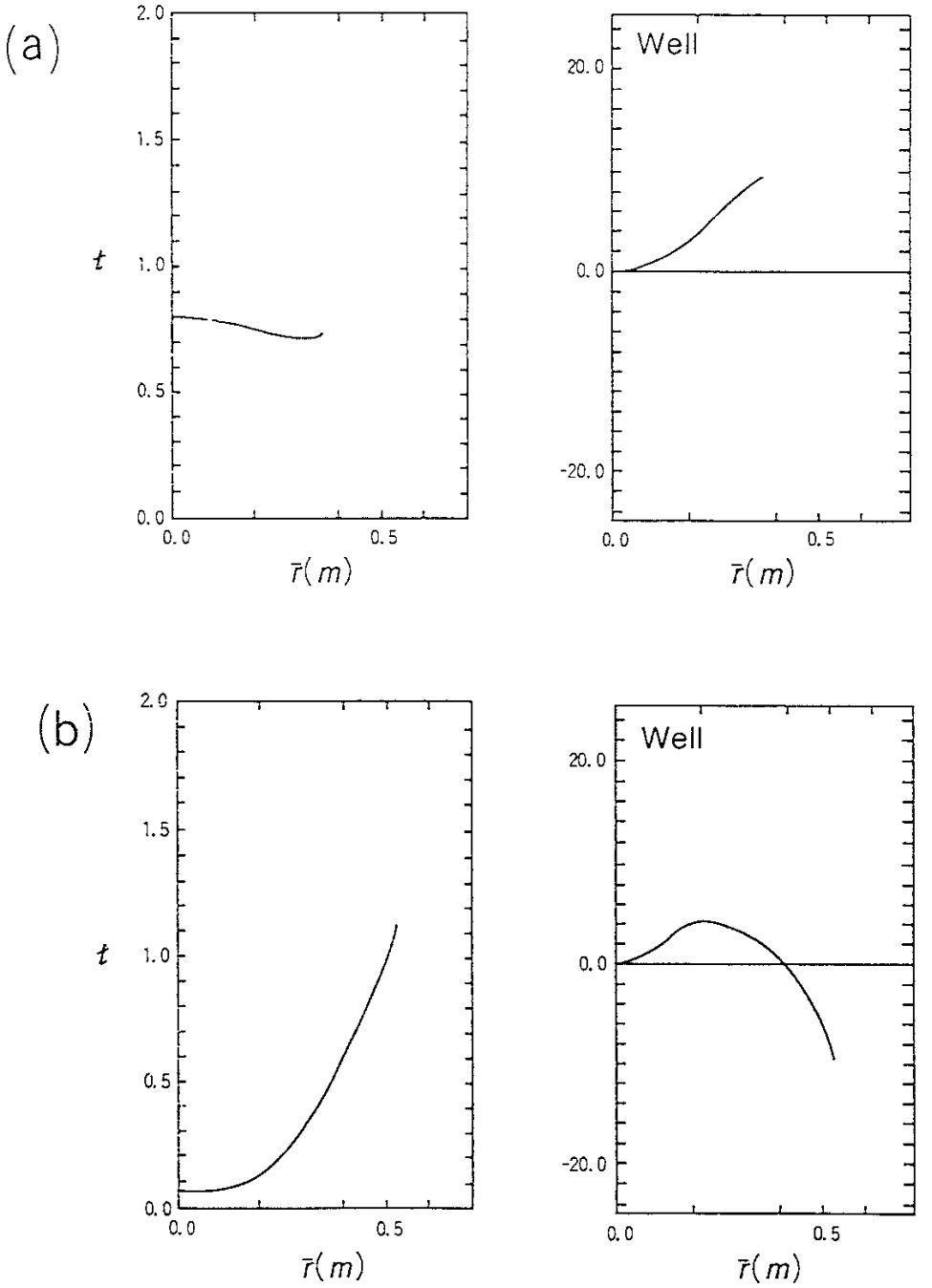
(a)
2.0
1.5
1.0
0.5
0.0
t
0.0
0.5
r̄(m)
Well
20.0
0.0
-20.0
0.0
0.5
r̄(m)
(b)
2.0
1.5
1.0
0.5
0.0
t
0.0
0.5
r̄(m)
Well
20.0
0.0
-20.0
0.0
0.5
r̄(m)

Fig.8

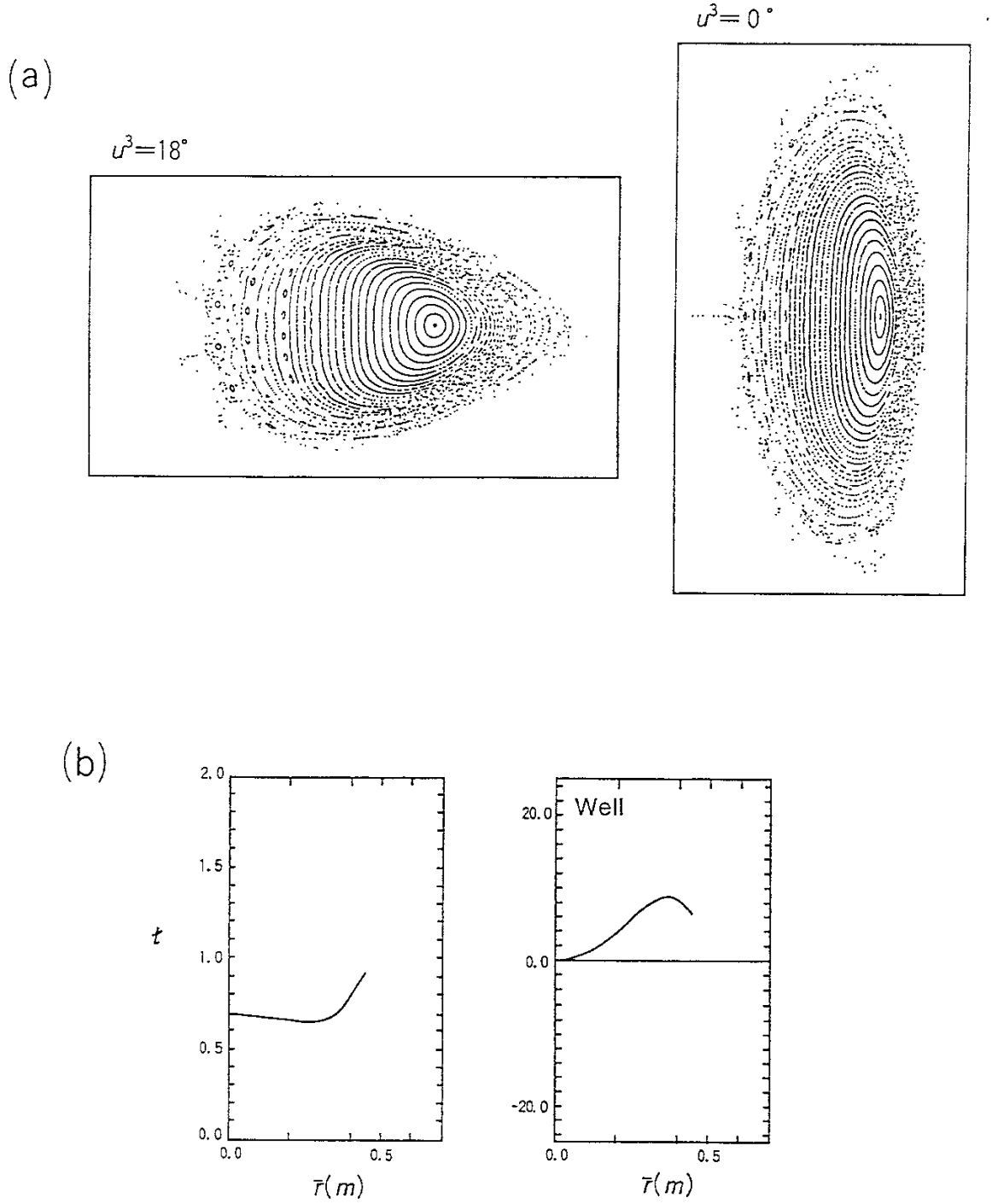
(a)
u^3=18°
u^3= 0 °
(b)
t
2.0
1.5
1.0
0.5
0.0
0.0
0.5
$\bar{r}$(m)
Well
20.0
0.0
-20.0
0.0
0.5
$\bar{r}$(m)

Fig.9

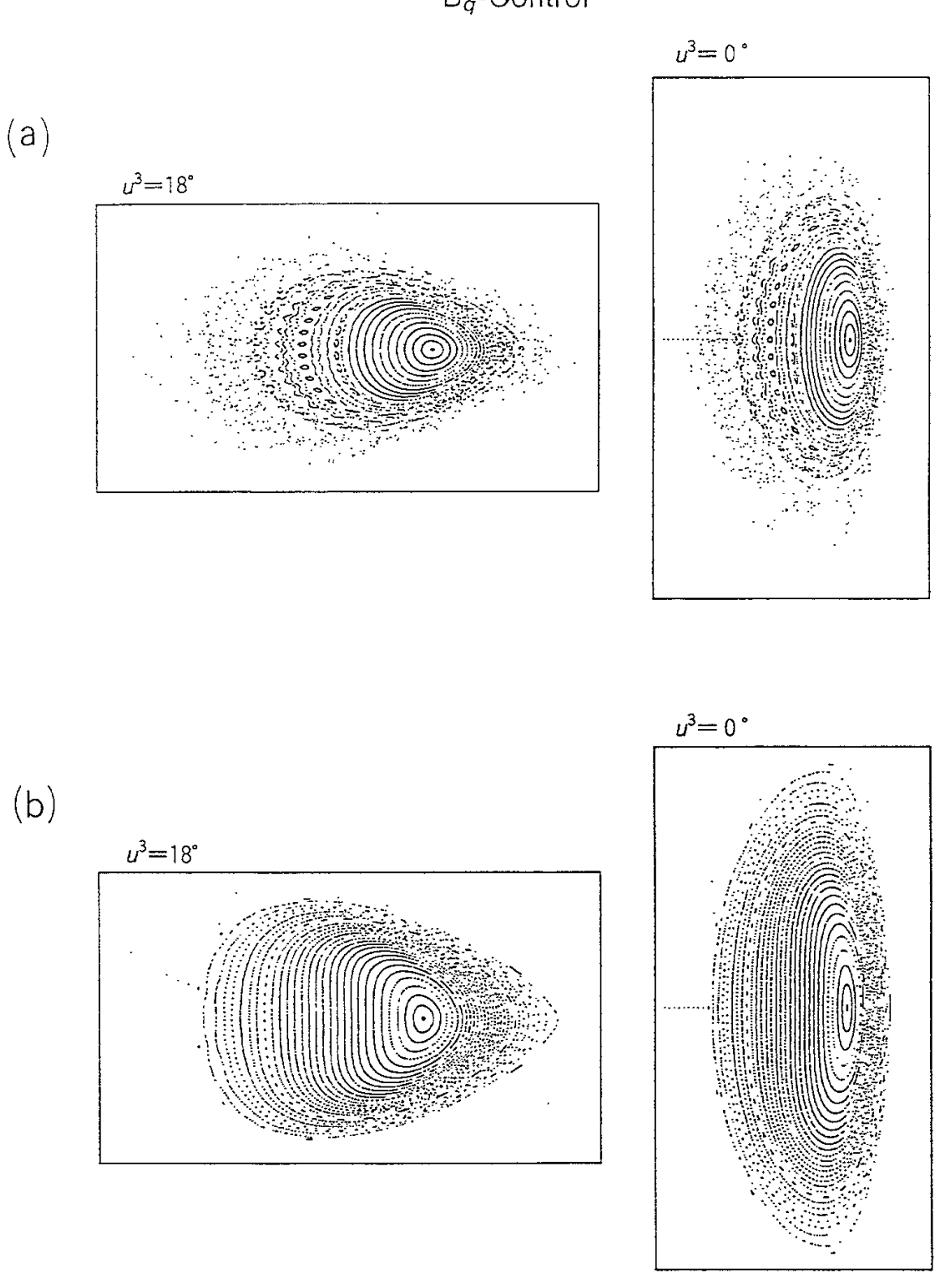

Fig.10

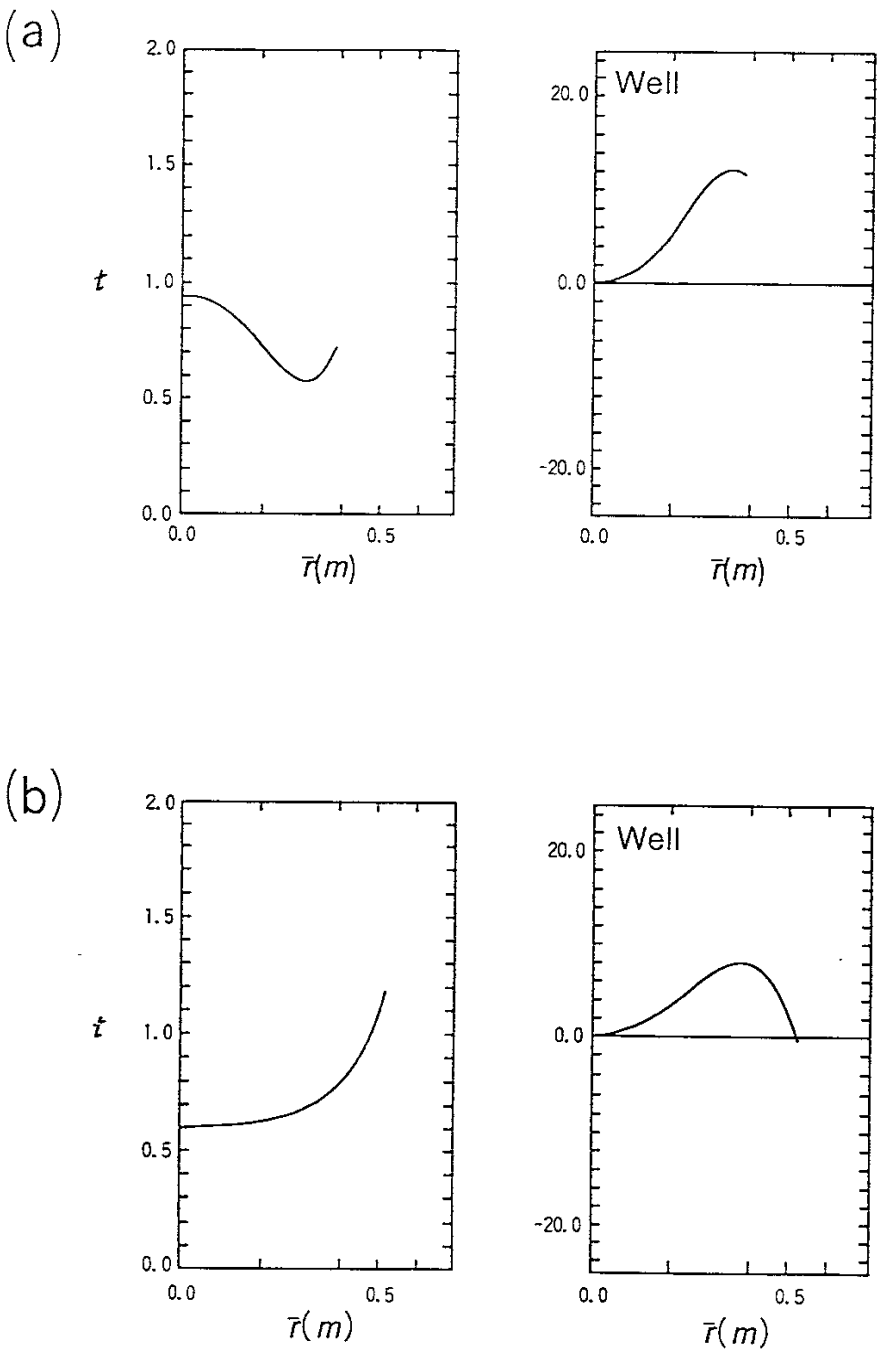
(a)
2.0
1.5
t
1.0
0.5
0.0
0.0
0.5
r̄(m)
20.0
Well
0.0
-20.0
0.0
0.5
r̄(m)
(b)
2.0
1.5
t
1.0
0.5
0.0
0.0
0.5
r̄(m)
20.0
Well
0.0
-20.0
0.0
0.5
r̄(m)

Fig.11

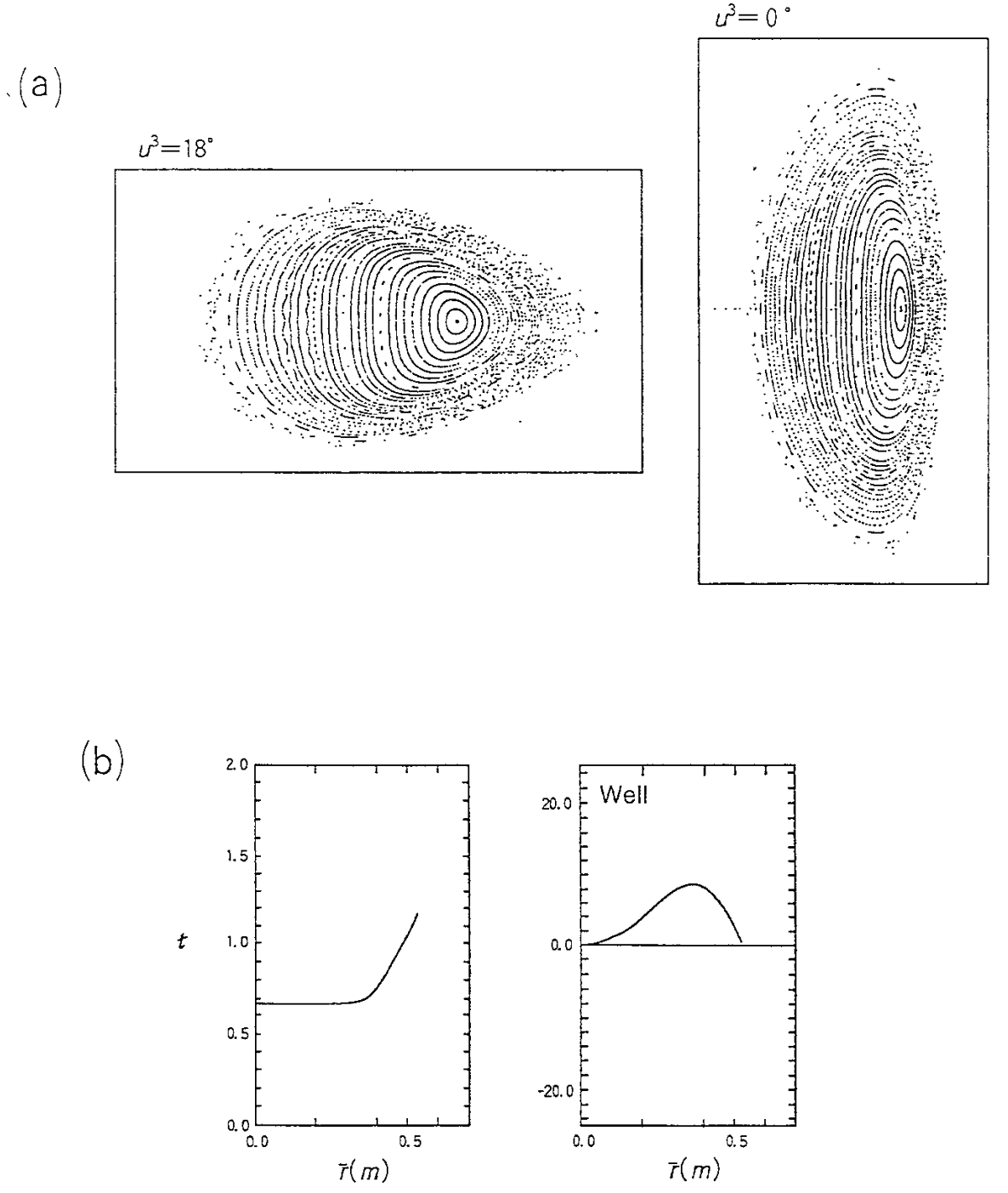
(a)
ζ^3=18°
ζ^3= 0 °
(b)
t
2.0
1.5
1.0
0.5
0.0
0.0
0.5
$\bar{r}(m)$
Well
20.0
0.0
-20.0
0.0
0.5
$\bar{r}(m)$

Fig.12

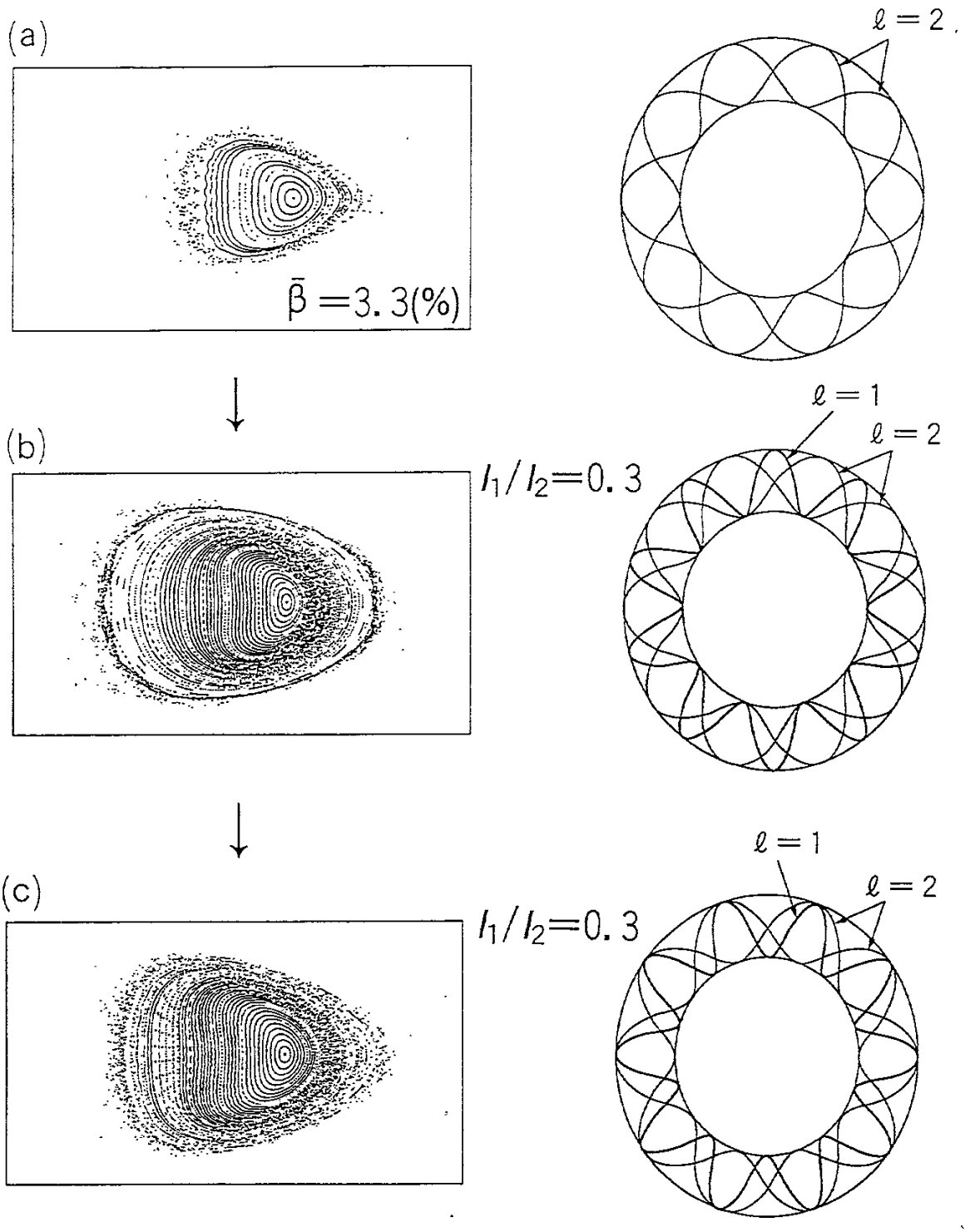

Fig.13

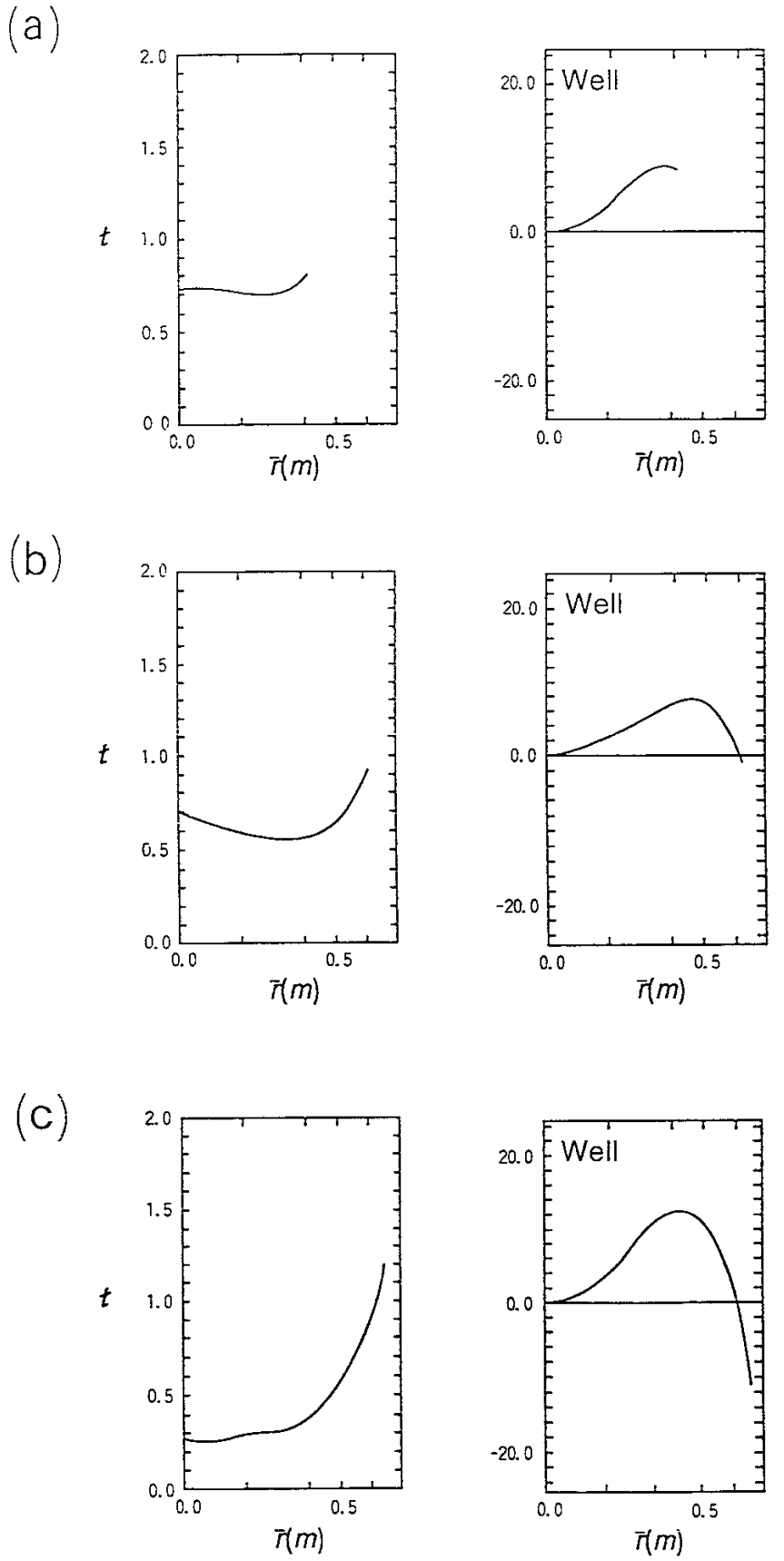
(a)
2.0
1.5
t
1.0
0.5
0.0
0.0
0.5
r̄(m)
20.0
Well
0.0
-20.0
0.0
0.5
r̄(m)
(b)
2.0
1.5
t
1.0
0.5
0.0
0.0
0.5
r̄(m)
20.0
Well
0.0
-20.0
0.0
0.5
r̄(m)
(c)
2.0
1.5
t
1.0
0.5
0.0
0.0
0.5
r̄(m)
20.0
Well
0.0
-20.0
0.0
0.5
r̄(m)

Fig.14

$I_{\ell=1}/I_{\ell=2} = -0.3$

(a)

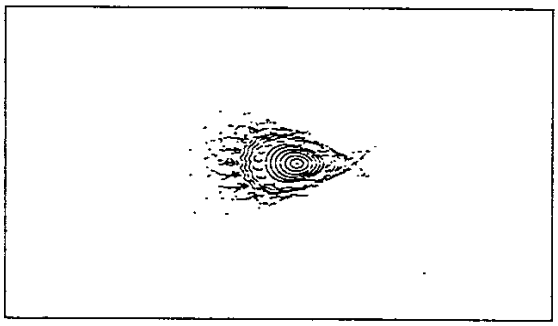

$I_{\ell=1}/I_{\ell=2} = 0.3$

(b)

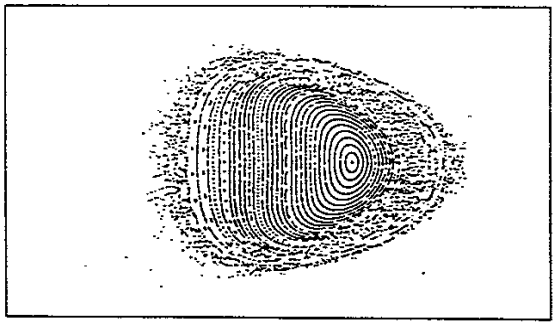

$I_{\ell=1}/I_{\ell=2} = 0.5$

(c)

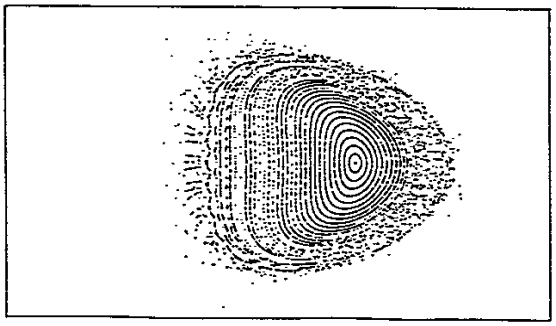

Fig.15

Recent Issues of NIFS Series

NIFS-72 S. -I. Itoh, H. Sanuki and K. Itoh, *Effect of Electric Field Inhomogeneities on Drift Wave Instabilities and Anomalous Transport* ; Jan. 1991

NIFS-73 Y.Nomura, Yoshi.H.Ichikawa and W.Horton, *Stabilities of Regular Motion in the Relativistic Standard Map*; Feb. 1991

NIFS-74 T.Yamagishi, *Electrostatic Drift Mode in Toroidal Plasma with Minority Energetic Particles,* Feb. 1991

NIFS-75 T.Yamagishi, *Effect of Energetic Particle Distribution on Bounce Resonance Excitation of the Ideal Ballooning Mode*, Feb. 1991

NIFS-76 T.Hayashi, A.Tadei, N.Ohyabu and T.Sato, *Suppression of Magnetic Surface Breading by Simple Extra Coils in Finite Beta Equilibrium of Helical System;* Feb. 1991

NIFS-77 N. Ohyabu, *High Temperature Divertor Plasma Operation*; Feb. 1991

NIFS-78 K.Kusano, T. Tamano and T. Sato, *Simulation Study of Toroidal Phase-Locking Mechanism in Reversed-Field Pinch Plasma*; Feb. 1991

NIFS-79 K. Nagasaki, K. Itoh and S. -I. Itoh, *Model of Divertor Biasing and Control of Scrape-off Layer and Divertor Plasmas*; Feb. 1991

NIFS-80 K. Nagasaki and K. Itoh, *Decay Process of a Magnetic Island by Forced Reconnection*; Mar. 1991

NIFS-81 K. Takahata, N. Yanagi, T. Mito, J. Yamamoto, O.Motojima and LHDDesign Group, K. Nakamoto, S. Mizukami, K. Kitamura, Y. Wachi, H. Shinohara, K. Yamamoto, M. Shibui, T. Uchida and K. Nakayama, *Design and Fabrication of Forced-Flow Coils as R&D Program for Large Helical Device*; Mar. 1991

NIFS-82 T. Aoki and T. Yabe, *Multi-dimensional Cubic Interpolation for ICF Hydrodynamics Simulation*; Apr. 1991

NIFS-83 K. Ida, S.-I. Itoh, K. Itoh, S. Hidekuma, Y. Miura, H. Kawashima, M. Mori, T. Matsuda, N. Suzuki, H. Tamai, T.Yamauchi and JFT-2M Group, *Density Peaking in the JFT-2M Tokamak Plasma with Counter Neutral Beam Injection* ; May 1991

NIFS-84 A. Iiyoshi, *Development of the Stellarator/Heliotron Research*; May 1991

NIFS-85 Y. Okabe, M. Sasao, H. Yamaoka, M. Wada and J. Fujita, *Dependence of Au^- Production upon the Target Work Function in a Plasma-Sputter-Type Negative Ion Source;* May 1991

NIFS-86 N. Nakajima and M. Okamoto, *Geometrical Effects of the Magnetic Field on the Neoclassical Flow, Current and Rotation in General Toroidal Systems*; May 1991

NIFS-87 S. -I. Itoh, K. Itoh, A. Fukuyama, Y. Miura and JFT-2M Group, *ELMy-H mode as Limit Cycle and Chaotic Oscillations in Tokamak Plasmas;* May 1991

NIFS-88 N.Matsunami and K.Kitoh, *High Resolution Spectroscopy of H^+ Energy Loss in Thin Carbon Film;* May 1991

NIFS-89 H. Sugama, N. Nakajima and M.Wakatani, *Nonlinear Behavior of Multiple-Helicity Resistive Interchange Modes near Marginally Stable States;* May 1991

NIFS-90 H. Hojo and T.Hatori, *Radial Transport Induced by Rotating RF Fields and Breakdown of Intrinsic Ambipolarity in a Magnetic Mirror*; May 1991

NIFS-91 M. Tanaka, S. Murakami, H. Takamaru and T.Sato, *Macroscale Implicit, Electromagnetic Particle Simulation of Inhomogeneous and Magnetized Plasmas in Multi-Dimensions;* May 1991

NIFS-92 S. - I. Itoh, *H-mode Physics, -Experimental Observations and Model Theories-, Lecture Notes, Spring College on Plasma Physics, May 27 - June 21 1991 at International Centre for Theoretical Physics (IAEA UNESCO) Trieste, Italy ;* Jun. 1991

NIFS-93 Y. Miura, K. Itoh, S. - I. Itoh, T. Takizuka, H. Tamai, T. Matsuda, N. Suzuki, M. Mori, H. Maeda and O. Kardaun, *Geometric Dependence of the Scaling Law on the Energy Confinement Time in H-mode Discharges;* Jun. 1991

NIFS-94 H. Sanuki, K. Itoh, K. Ida and S. - I. Itoh, *On Radial Electric Field Structure in CHS Torsatron / Heliotron;* Jun. 1991

NIFS-95 K. Itoh, H. Sanuki and S. - I. Itoh, *Influence of Fast Ion Loss on Radial Electric Field in Wendelstein VII-A Stellarator;* Jun. 1991

NIFS-96 S. - I. Itoh, K. Itoh, A. Fukuyama, *ELMy-H mode as Limit Cycle and Chaotic Oscillations in Tokamak Plasmas;* Jun. 1991

NIFS-97 K. Itoh, S. - I. Itoh, H. Sanuki, A. Fukuyama, *An H-mode-Like Bifurcation in Core Plasma of Stellarators;* Jun. 1991

NIFS-98 H. Hojo, T. Watanabe, M. Inutake, M. Ichimura and S. Miyoshi, *Axial Pressure Profile Effects on Flute Interchange Stability in the Tandem Mirror GAMMA 10;* Jun. 1991

NIFS-99 A. Usadi, A. Kageyama, K. Watanabe and T. Sato, *A Global Simulation of the Magnetosphere with a Long Tail : Southward and Northward IMF;* Jun. 1991

NIFS-100 H. Hojo, T. Ogawa and M. Kono, *Fluid Description of Ponderomotive Force Compatible with the Kinetic One in a Warm Plasma* ; July 1991

NIFS-101 H. Momota, A. Ishida, Y. Kohzaki, G. H. Miley, S. Ohi, M. Ohnishi K. Yoshikawa, K. Sato, L. C. Steinhauer, Y. Tomita and M. Tuszewski *Conceptual Design of D-^{3}He FRC Reactor "ARTEMIS"* ; July 1991

NIFS-102 N. Nakajima and M. Okamoto, *Rotations of Bulk Ions and Impurities in Non-Axisymmetric Toroidal Systems* ; July 1991

NIFS-103 A. J. Lichtenberg, K. Itoh, S. - I. Itoh and A. Fukuyama, *The Role of Stochasticity in Sawtooth Oscillation* ; Aug. 1991

NIFS-104 K. Yamazaki and T. Amano, *Plasma Transport Simulation Modeling for Helical Confinement Systems;* Aug. 1991

NIFS-105 T. Sato, T. Hayashi, K. Watanabe, R. Horiuchi, M. Tanaka, N. Sawairi and K. Kusano, *Role of Compressibility on Driven Magnetic Reconnection ;* Aug. 1991

NIFS-106 Qian Wen - Jia, Duan Yun - Bo, Wang Rong - Long and H. Narumi, *Electron Impact Excitation of Positive Ions - Partial Wave Approach in Coulomb - Eikonal Approximation* ; Sep. 1991

NIFS-107 S. Murakami and T. Sato, *Macroscale Particle Simulation of Externally Driven Magnetic Reconnection;* Sep. 1991

NIFS-108 Y. Ogawa, T. Amano, N. Nakajima, Y. Ohyabu, K. Yamazaki, S. P. Hirshman, W. I. van Rij and K. C. Shaing, *Neoclassical Transport Analysis in the Banana Regime on Large Helical Device (LHD) with the DKES Code;* Sep. 1991

NIFS-109 Y. Kondoh, *Thought Analysis on Relaxation and General Principle to Find Relaxed State;* Sep. 1991

NIFS-110 H. Yamada, K. Ida, H. Iguchi, K. Hanatani, S. Morita, O. Kaneko, H. C. Howe, S. P. Hirshman, D. K. Lee, H. Arimoto, M. Hosokawa, H. Idei, S. Kubo, K. Matsuoka, K. Nishimura, S. Okamura, Y. Takeiri, Y. Takita and C. Takahashi, *Shafranov Shift in Low-Aspect-Ratio Heliotron / Torsatron CHS* ; Sep 1991

NIFS-111 R. Horiuchi, M. Uchida and T. Sato, *Simulation Study of Stepwise Relaxation in a Spheromak Plasma ;* Oct. 1991

NIFS-112 M. Sasao, Y. Okabe, A. Fujisawa, H. Iguchi, J. Fujita, H. Yamaoka and M. Wada, *Development of Negative Heavy Ion Sources for Plasma Potential Measurement* ; Oct. 1991

NIFS-113 S. Kawata and H. Nakashima, *Tritium Content of a DT Pellet in Inertial Confinement Fusion* ; Oct. 1991

NIFS-114 M. Okamoto, N. Nakajima and H. Sugama, *Plasma Parameter Estimations for the Large Helical Device Based on the Gyro-Reduced Bohm Scaling* ; Oct. 1991

NIFS-115 Y. Okabe, *Study of Au^- Production in a Plasma-Sputter Type Negative Ion Source* ; Oct. 1991

NIFS-116 M. Sakamoto, K. N. Sato, Y. Ogawa, K. Kawahata, S. Hirokura, S. Okajima, K. Adati, Y. Hamada, S. Hidekuma, K. Ida, Y. Kawasumi, M. Kojima, K. Masai, S. Morita, H. Takahashi, Y. Taniguchi, K. Toi and T. Tsuzuki, *Fast Cooling Phenomena with Ice Pellet Injection in the JIPP T-IIU Tokamak;* Oct. 1991

NIFS-117 K. Itoh, H. Sanuki and S. -I. Itoh, *Fast Ion Loss and Radial Electric Field in Wendelstein VII-Λ Stellarator*; Oct. 1991

NIFS-118 Y. Kondoh and Y. Hosaka, *Kernel Optimum Nearly-analytical Discretization (KOND) Method Applied to Parabolic Equations <<KOND-P Scheme>>;* Nov. 1991

NIFS-119 T. Yabe and T. Ishikawa, *Two- and Three-Dimensional Simulation Code for Radiation-Hydrodynamics in ICF*; Nov. 1991

NIFS-120 S. Kawata, M. Shiromoto and T. Teramoto, *Density-Carrying Particle Method for Fluid* ; Nov. 1991

NIFS-121 T. Ishikawa, P. Y. Wang, K. Wakui and T. Yabe, *A Method for the High-speed Generation of Random Numbers with Arbitrary Distributions;* Nov. 1991

NIFS-122 K. Yamazaki, H. Kaneko, Y. Taniguchi, O. Motojima and LHD Design *Group, Status of LHD Control System Design ; Dec. 1991*

NIFS-123 Y. Kondoh, *Relaxed State of Energy in Incompressible Fluid and Incompressible MHD Fluid* ; Dec. 1991

NIFS-124 K. Ida, S. Hidekuma, M. Kojima, Y. Miura, S. Tsuji, K. Hoshino, M. Mori, N. Suzuki, T. Yamauchi and JFT-2M Group, *Edge Poloidal Rotation Profiles of H-Mode Plasmas in the JFT-2M Tokamak ;* Dec. 1991

NIFS-125 H. Sugama and M. Wakatani, *Statistical Analysis of Anomalous Transport in Resistive Interchange Turbulence* ;Dec. 1991

NIFS-126 K. Narihara, *A Steady State Tokamak Operation by Use of Magnetic Monopoles* ; Dec. 1991

NIFS-127 K. Itoh, S. -I. Itoh and A. Fukuyama, *Energy Transport in the Steady State Plasma Sustained by DC Helicity Current Drive* ;Jan. 1992

NIFS-128 Y. Hamada, Y. Kawasumi, K. Masai, H. Iguchi, A. Fujisawa, JIPP T-IIU Group and Y. Abe, *New Hight Voltage Parallel Plate Analyzer* ; Jan. 1992

NIFS-129 K. Ida and T. Kato, *Line-Emission Cross Sections for the Charge-exchange Reaction between Fully Stripped Carbon and Atomic Hydrogen in Tokamak Plasma*; Jan. 1992